Environ Monit Assess (2019) 191: 462
https://doi.org/10.1007/s10661-019-7580-3

Using time-series Sentinel-1 data for soil prediction on invaded coastal wetlands

Ren-Min Yang · **Wen-Wen Guo**

Received: 9 January 2019 / Accepted: 4 June 2019 / Published online: 25 June 2019
© Springer Nature Switzerland AG 2019

Abstract Coastal soils are particularly sensitive to nonnative species invasion. In this context, spatially explicit soil information is essential for improving the knowledge of the role of soil in changing environments, supporting coastal sustainable management. Synthetic-aperture radar (SAR) data provides an attractive opportunity to monitor soil because the acquisition of images is independent of weather and daylight. However, SAR has not been commonly used for soil prediction. In this study, we firstly investigated the temporal variation of vegetation canopy and the soil-vegetation relationship using Sentinel-1 data in an invaded coastal wetland. And then we built 3D models to predict soil properties at multiple depths. A total of 16 Sentinel-1 images were acquired in a growing season. A series of soil physicochemical properties were examined including soil bulk density, texture, organic/inorganic carbon, pH, salinity, total nitrogen, and C/N ratio, relating to three depth layers in the top 1-m depth. Our results showed that time-series Sentinel-1 data can capture temporal characteristics of vegetation, and VH/VV was more sensitive to the vegetation growth than VH and VV. The soil-vegetation relationship captured by time-series SAR data was beneficial to predict soil properties, especially for soil chemical properties. The models provided permissible prediction accuracy, with an average RPD of 0.99. We concluded that the prior understanding of the temporal variation of SAR data is essential for developing practical soil prediction strategy. Our results highlight that SAR has the potential to predict a diverse set of soil properties in coastal wetlands with dense vegetation cover.

Keywords Soil monitoring · Time-series Sentinel-1 imagery · 3D model · Coastal restoration · Soil-vegetation relationship

R.-M. Yang (✉)
School of Geography, Geomatics, and Planning, Jiangsu Normal University, Xuzhou 221116, China
e-mail: yangrenmincs@163.com

W.-W. Guo
Department of Tourism, Resources and Environment, Zaozhuang University, Zaozhuang 277160, China
e-mail: wwaxmt@163.com

Introduction

Coastal wetlands are important regions that provide important ecosystem services including carbon sequestration and flooding resistance. However, they are threatened by nonnative species invasion that is altering the structure and service of ecosystems worldwide. The soils of coastal wetlands, for instance, are particularly sensitive to the invasion, where soil physicochemical properties could be substantially altered regarding the expansion of nonnative species into areas that lack native species (Yang and Guo 2018). Invasion-induced soil changes are important indicators for global warming potential, due to the role the nonnative species plays in regulating the interaction between soil and climate change (Yuan et al. 2015). Thus, a better understanding

of soil patterns is of great importance for coping with the invasive impact and maintaining sustainable management of coastal wetlands.

The use of remote sensing as a primary data source is an exciting area for soil quantification research because they can provide timely spatial-temporal information on soil status economically (Mulder et al. 2011). Furthermore, improvements in newly released and forthcoming imagers (i.e., Sentinel 1-2-3, Landsat 8 OLI, EnMAP, and HyspIRI) are attracting scientists to employ remote sensing techniques in estimating soil properties, while these new sensors may pose significant challenges in relating remotely sensed information to soils. Given this background, it is necessary to achieve an understanding of remote sensing data in indicating the spatial variation of soil properties.

In the past few years, a variety of remote sensing data, including optical data and synthetic-aperture radar (SAR) data, have been heavily tested to explore the relationships between image signals and soil components (e.g., Metternicht and Zinck 2003; Vaudour et al. 2013; Araya et al. 2016; Demattê et al. 2017; Han et al. 2017). The applications of optical images in soil prediction have been widely reported, but the presence of clouds affects the quality of these data, and it is frequently a problem for the analysis. Compared to optical data, SAR ensures the acquisition of images independent of weather and daylight, offering the opportunity to monitor variations of soil consistently. The use of SAR in the quantitative estimation of soil properties depends on the sensitivity of backscatter coefficients to changes in soil moisture and land surface conditions (Kasischke et al. 1997). For this reason, SAR data are primarily used for quantitative estimation of soil moisture (e.g., Dubois et al. 1995; Schuler et al. 2002; Han et al. 2017), and it has not been commonly used for predicting broader sets of soil properties such as soil carbon, nitrogen, texture, and pH.

The applications of SAR data relating to soil properties have been conducted for bare soil as well as vegetation-covered soil. Penetration capability of SAR backscatter from long wavelengths, such as P-band and L-band SAR datasets, has been demonstrated in the case of vegetation-covered soil (Freeman and Durden 1998; Srivastava et al. 2006). However, the penetration capability of short wavelengths concerning the vegetation cover is restricted to the top layers, such as Sentinel-1 that is a new C-band SAR satellite launched in April 2014. There are still some issues about the application of SAR data in soil prediction in areas with dense vegetation such as salt marsh. We noted that recent studies (e.g., Solon et al. 2012; Anne et al. 2014; Yang et al. 2015; Demattê et al. 2017) had explored the possible relationship between soil and plant-life through remote sensing techniques, suggesting that there is a close relationship between soil and vegetation. In our case study, the introduction of *Spartina alterniflora* Loisel. (*S. alterniflora*) substantially influenced plant characteristics such as plant community and structure (Li et al. 2009). As a result, some soil chemical properties were significantly changed in response to *S. alterniflora* invasion such as carbon storage, soil pH, and salinity (Yang and Guo 2018). In addition, they found that some physical properties may also be altered following *S. alterniflora* invasion. For example, developed a rooting system of *S. alterniflora* may loosen the soil through influencing soil physical structure such as bulk density and porosity. Some studies, such as Sarti et al. (2017) and Veloso et al. (2017), have exploited the sensitivity of SAR data to vegetation, implying that vegetation characteristics can be detected from time-series SAR imagery. These studies indicate that soil chemical and physical properties might be indirectly related to SAR data by identifying vegetation. Nevertheless, there is less concern about the soil-vegetation relationship based on SAR backscatter data.

Most of previous soil mapping studies focused on the surface with the soil depth up to 10–30 cm (Minasny et al. 2013). However, a large amount of uncertainty exists within soil properties at deeper layers (Batjes 1996; Jobbagy and Jackson 2000). In coastal wetlands, Yang and Guo (2018) found that *S. alterniflora* invasion led to the substantial decline in soil salinity throughout the 1 m depth soil. Following the short-term invasion of *S. alterniflora*, soil properties may be significantly different between different depth layers such as water content, bulk density, pH, and organic carbon (Feng et al. 2017). Therefore, detailed soil information in depth is vital for evaluating the effects of *S. alterniflora* invasion on soils. It is also useful for accessing ecosystem services and wetland management because coastal wetland soils play an important role on regulating the biogeochemical and physical processes such as filtering of pollutants, water inflow, plant succession, and microbial function (Berkowitz et al. 2018). Therefore, the

variability of soil properties in depth should be given great consideration.

To model the realistic distribution of soil properties in both vertical and lateral dimensions, some attempts have been made (e.g., Meersmans et al. 2009; Mishra et al. 2009; Adhikari et al. 2014; Veronesi et al. 2014; Poggio and Gimona 2014). These studies combined a variety of spatial prediction models such as geostatistical models, fuzzy logical models, Cubist, and neural network models. These models usually have a complex structure and hard to interpret. Instead, linear models have lower complexity and higher interpretability and thus they are still useful in soil prediction. However, linear models with a large number of variables (i.e., time-series Sentinel-1 variables used in this study) may be overfitted and lead to low prediction accuracy. The least absolute shrinkage and selection operator (lasso) penalized-regression model provides an optimal solution to resist overfitting (Tibshirani 1996). Lasso is a regularization regression method that estimates linear model parameters by penalizing model complexity and setting coefficients of irrelevant to be zero, which can produce interpretable models with accurate predictions. Recently, lasso has been successfully used for soil predictions (e.g., Liddicoat et al. 2015; Nussbaum et al. 2018; Pejović et al. 2018).

In this study, we aimed to evaluate the capacity of time-series SAR data in indicating spatial patterns of soil physicochemical properties related to depths in an invaded ecosystem in the east-central China coast. In this way, two specific objectives were set to investigate (1) the correlation between SAR indices and diverse set of soil properties and (2) SAR-based 3D models of soil properties for spatial prediction using lasso. We hypothesized that time-series SAR data could reflect the dynamics of vegetation canopies that were assumed to indicate soil variations. In terms of correlations observed between the deeper soil and SAR data, they should rely on the interconnection between the upper layer and the lower layer because of the direct effect of the plant on soils dominated at the surface layer. This study was expected to not only expand the existing knowledge about the relationship between SAR data and a limited set of soil properties but also provide evidence to improve soil monitoring strategy for coastal wetland conservation.

Materials and methods

Study area

The study site is located on the coastline of east-central China, covering an area of approximately 17 km^2 (Fig. 1). The area is part of the buffer region of the Jiangsu Yancheng Wetland Natural Reserve, Rare Birds, which is one of the first coastal wetland nature reserves in China. The climate in the region is characterized by hot and wet summers and cold winters. Mean annual temperatures range from 13.7–14.6 °C and mean annual precipitation is about 1000 mm, and most of the rain falls from June through September. Plants are quite homogeneous and are dominated by *S. alterniflora*, which is an exotic species introduced into this intertidal zone since 1980s. *S. alterniflora* is a rhizomatous perennial grass with a dense root system and has a rapid reproduction (Li et al. 2009). Before introducing *S. alterniflora*, this was a mudflat region. Soils are poorly drained and dominantly by Gleyic Solochaks (IUSS Working Group WRB 2015).

Soil sampling and analysis

To present the soil-vegetation relationship, a soil sampling strategy was designed based on a space-for-time substitution method, which has been proven to be an efficient method to represent the temporal variation of soils in response to *S. alterniflora* invasion (Gao et al. 2016; Feng et al. 2017). Detailed information about the sampling has been documented by Yang and Guo (2018). Briefly, a stratification of plant settlement stages was conducted using a time series of Landsat imagery from the United States Geological Survey (USGS). Furthermore, a total of 15 sites were randomly selected along five coastal transects according to settlement stages. At each location, soil samples were collected from the three soil layers 0–30 cm, 30–60 cm, and 60–100 cm. The sampling method was expected to guarantee correlations between soil and vegetation because a space-for-time method ensures us to fill gaps in temporal records using spatial data. Therefore, samples collected using this method can capture temporal relationships between soil and vegetation.

Soil properties examined in the study include bulk density, texture, salinity, pH, organic carbon,

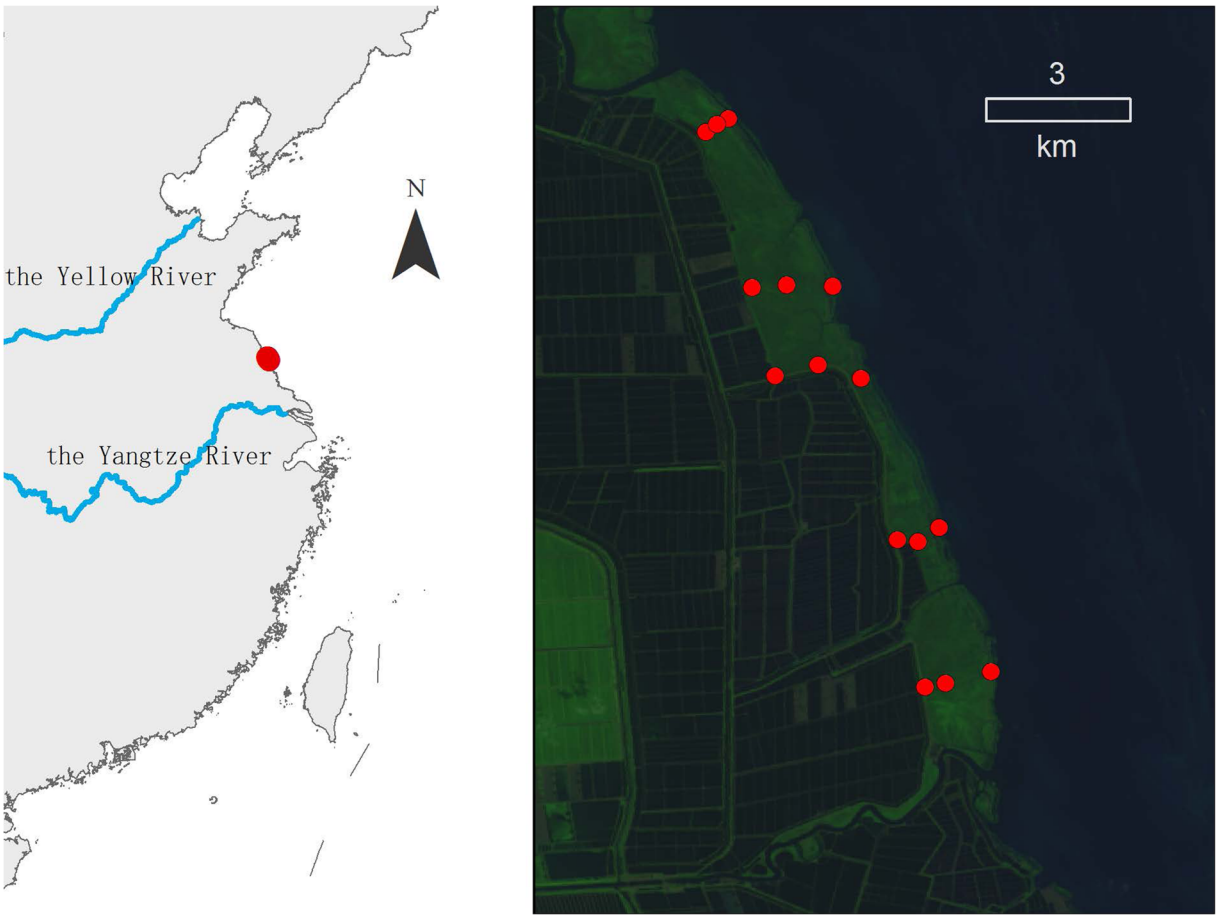

Fig. 1 Location of the study area of a coastal wetland in east-central China. The red points indicate the locations of soil sampling sites

inorganic carbon, total nitrogen, and C/N ratio. Soil bulk density (BD, g cm^{-3}) was the dry weight of soil divided by the total soil volume from a core sample with a 5-cm diameter and 5-cm depth. Particle-size fractions were determined by a laser diffraction particle-size analyzer (LS230, Beckman Coulter, Fullerton, CA, USA). Soil salt content (salinity, g kg^{-1}) was measured by the electric conductivity and the dry evaporation method (Rhoades and Ingvalson 1971). Soil pH was measured using a 1:2.5 soil-solution ratio. Soil organic carbon concentration (SOC, g kg^{-1}) was determined using the Walkley-Black wet combustion method (Nelson and Sommers 1982). Soil inorganic carbon concentration (SIC, g kg^{-1}) was determined using a modified pressure transducer method (Sherrod et al. 2002). Soil total nitrogen (TN, g kg^{-1}) was measured using an automatic Kjeldahl digestion apparatus (Kjeltec 8400, Foss, Denmark). Finally, the carbon-to-nitrogen ratio (C/N) was calculated.

Sentinel-1 imagery and ancillary data

The Sentinel-1 mission is the part of the Global Monitoring for Environment and Security (GMES) program of the European Union (EU) and the European Space Agency (ESA). They have provided continuous C-band SAR data to support environmental monitoring applications, such as land surface change and marine research (Attema et al. 2007). Sentinel-1 offers global coverage of the earth surface every 12 days with Sentinel-1A and 6 days combined with Sentinel-1B. A total of 16 Sentinel-1A images from vegetation growing season (Apr to Oct in 2017) have been acquired from ESA (freely available from https://scihub.copernicus.eu/), while Sentinel-1B data was not available across the area. These ascending images were pre-defined using the

interferometric wide swath (IW) mode with two polarization channels (VV and VH). The Sentinel-1A scenes were acquired as Level-1 Ground Range Detected (GRD) products that consist of focused SAR data that has been detected, multi-looked, and projected to the ground range using an Earth ellipsoid model.

SAR data was processed in the Sentinel Toolbox SNAP (ESA 2017). Calibration was firstly performed for each image to reduce radiometric errors and to transfer DN values to backscatter coefficients in dB. Then, multi-looking with a 3×3 window size was applied to diminish the effect of speckle noise, creating a spatial resolution of 20-m data. Additionally, the geometric correction was used to correct SAR image geometric distortions using the digital elevation model from the Shuttle Radar Topography Mission. For additional information on the land surface, the ratio VH/VV and VH and VV were used in time-series analysis of vegetation for soil estimation. The ratio VH/VV probably reduces system and environmental errors and might be a more stable indicator in temporal analysis than VH and VV (Veloso et al. 2017). Furthermore, multi-temporal features were extracted from time-series data at three polarizations, including gradient (grad), maximum (max), maximum decrement (maxd), maximum increment (maxi), maximum ratio (maxr), mean (mea), median (med), minimum (min), minimum ratio (minr), span difference (spand), span ratio (spanr), and standard deviation (std).

The time series of SAR backscatters were analyzed with the support of normalized difference vegetation index (NDVI) and soil moisture content, which were obtained from the Google Earth Engine (GEE) platform. For this study, a product of a Moderate Resolution Imaging Spectroradiometer (MODIS) combined 8-day NDVI was used. Surface 10-cm moisture data (kg m^{-2}) was derived from Global Land Data Assimilation System (GLDAS) datasets at a time scale of 3 h. The temporal resolution of NDVI and soil moisture were rescaled by Sentinel-1A data.

Correlation analysis

The logarithmic form of SAR indices and soil properties were used for statistical analysis. Pearson correlation analysis was used to analyze the relationships between soil properties and SAR backscatters and temporal features. A significant correlation coefficient (r) was considered at the $P < 0.05$ level.

3D modeling of soil properties

For prediction purposes, we used the least absolute shrinkage and selection operator (lasso) penalized-regression model to build 3D models that use SAR indices and depth as covariates. The interactions between SAR indices and depth were also included in 3D models, assuming that the effect of predictors varies with depth. Lasso has the capacity to select the optimal set of predictors from a large number of variables and improve prediction accuracy through shrinking coefficient values. Non-important variables with coefficients shrunken to zero would be excluded from the model. The strength of penalty in lasso is controlled by a regularization parameter λ. We used the R package glmnet (R Core Team 2017; Friedman et al. 2010) to perform lasso prediction models. For each soil property, the optimal λ value was determined by performing a built-in cross-validation option. The optimal regression coefficients corresponded to the least complex model with error within one standard error of the minimum cross-validated mean squared error (Hastie et al. 2009).

The model performance was evaluated by leave-one-out cross-validation (LOOCV) where one sample in each depth layer was randomly selected for each LOOCV. RPD (a ratio of performance to deviation) was used to evaluate the model fit. Here, a RPD value larger than one was used to imply that there is a model improvement.

Results and discussion

Soil physicochemical characteristics

The mean and coefficient of variation (CV) values of BD, clay, sand, silt, C/N, pH, salinity, SIC, SOC, and TN are presented in Table 1. The results show that soil bulk density did not change much with years under the invasion of *S. alterniflora* with small CV values. The variability of BD in the three soil layers was slight. Bulk density in the coastal region was mainly determined by increasing seaward rates of mineral sedimentation and organic matter accumulation from vegetation (Wang et al. 2016a, b). *S. alterniflora* had a more significant influence on sand contents than clay and silt contents with CV value of 51.89% at 0–100 cm. Most of the soil textures were silt loams in the top 1-m depth.

Table 1 Mean and coefficient of variation (CV) of soil properties

Soil attributes	0–30 cm		30–60 cm		60–100 cm		0–100 cm	
	Mean	CV (%)	Mean	CV (%)	Mean	CV (%)	Mean	CV (%)
BD (g cm^{-3})	1.25	8.80	1.25	17.60	1.28	13.28	1.26	13.49
Clay (%)	12.53	25.78	14.19	22.41	12.33	26.76	13.02	25.12
Sand (%)	19.72	50.15	15.22	46.58	21.32	53.05	18.75	51.89
Silt (%)	67.75	10.94	70.59	6.26	66.35	12.84	68.23	10.36
C/N	12.26	14.19	13.44	17.11	11.07	13.73	12.26	16.97
pH	8.55	3.51	8.55	2.22	8.66	1.73	8.57	2.57
Salinity (g kg^{-1})	10.24	48.24	10.66	48.78	9.22	36.01	10.04	44.82
SIC (g kg^{-1})	11.40	15.96	11.96	12.88	11.36	10.92	11.57	13.31
SOC (g kg^{-1})	7.37	18.72	6.38	26.02	4.39	37.59	6.05	32.73
TN (g kg^{-1})	0.61	18.03	0.48	25.00	0.39	33.33	0.49	30.61

The mean soil pH ranged from 8.55 to 8.66 for the three layers, and the spatial variation was very minimal (CV, 1.73–3.51%). Due to the plant succession in reducing tidal flooding, soil salt content decreased as the growth of salt marsh (Gedan et al. 2009). Soil salinity contents were similar for the three layers (Table 1), but the spatial variation was moderate with CV values fell within the 36.01–48.78% range. Soils in the entire area had low SOC and TN concentration levels. The mean SOC and TN concentrations decreased as depth increased as expected. Concentrations of SOC and TN were most variable in 60–100 cm, CV values in the top 100 cm increased with soil depth to about 37.59% for SOC and 33.33% for TN. The variability of SOC and TN was a result of the enhanced ability of C and N accumulation by *S. alterniflora* invasion (Yang et al. 2017). The C/N and SIC presented a low degree of spatial variability in lateral and vertical directions.

Time-series characteristics of SAR backscatter

The time series of SAR backscatters (VH, VV, and VH/VV) were presented in Fig. 2. It can be observed that some correlations exist between SAR backscatters and the corresponding time series of NDVI and soil moisture at a glance, although the profiles of VH, VV, and VH/VV showed complex variations. It seems that VH/VV was more sensitivity to *S. alterniflora* than VH and VV because there is a good agreement between VH/VV and NDVI after the vegetation returns to green (from 27 Jun to 28 Aug).

At the beginning stage of the growing season (from 04 Apr to 27 Jun), although VH/VV presented complex variations, the profile of VH/VV can be correlated to the variation of NDVI. For example, a slight increase of NDVI was observed from 16 Apr to 28 Apr, which was followed by the increasing VH/VV backscatter. Then, a small variation of NDVI was presented in the profile of VH/VV until the beginning of June. The observed pattern variations of VH and VV backscatters and their poor relationships to NDVI can be explained by the effects of soil moisture. A stable correlation between NDVI and VH/VV backscatters was observed from the end of June to the end of August. As a result of the increasing chlorophyll, the observed relationship was related to the sensitivity of VH/VV to fresh biomass (Veloso et al. 2017). At this stage, a decrease of VH and VV backscatters was observed until the beginning of August. It is probably because VH and VV backscatters were attenuated by the increasing volume fraction of vegetation (Brown et al. 2003; Jia et al. 2013). These findings illustrated that there was a potential of Sentinel-1A data to capture the temporal behavior of coastal vegetation. However, the temporal profiles of VH/VV, VH, and VV were not similar, and the ability to indicate vegetation variations of three polarizations was influenced by the contribution from the canopy and ground, such as soil moisture content and vertical structure of the plant.

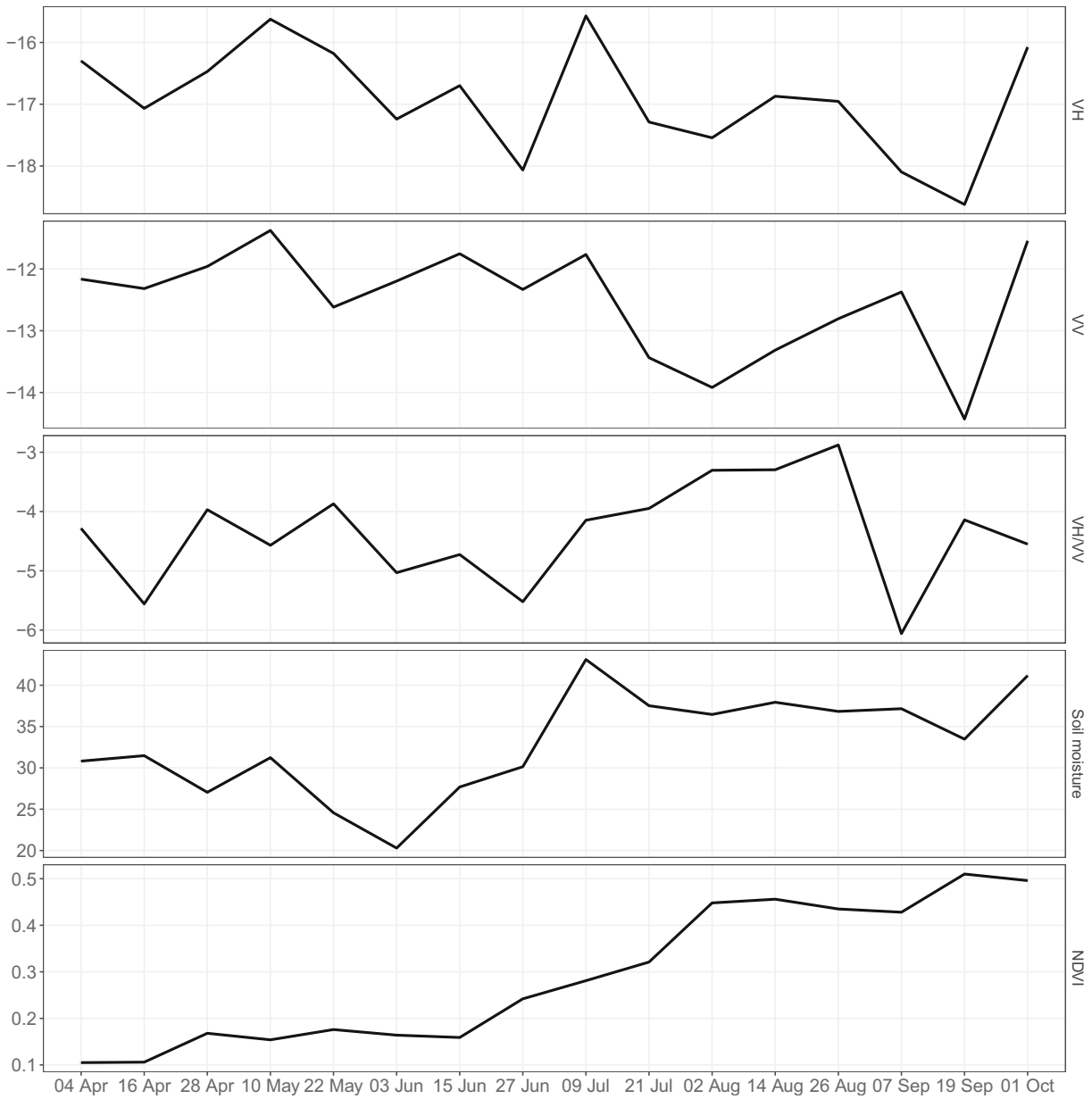

Fig. 2 Plots of temporal variations of mean values of VH, VV, VH/VV, soil moisture content, and NDVI over the study area

Spatial-temporal correlations between soil properties and SAR indices

Some significant ($P < 0.05$) relationships between soil properties and SAR backscatters (VH/VV, VH, and VV) and multi-temporal features were observed (Figs. 3 and 4). The r values related to SAR backscatters presented considerably large variations during a growing season, indicating the unstable relationships between soil and SAR backscatters. Most of their differences can be explained by fluctuations in SAR backscatters. As discussed before, VH/VV, VH, and VV were mostly affected by variations in the soil and vegetation. For example, the dynamics of soil moisture content driven by rainfall and tidal movements may cause the increase of VH and VV backscatters (Fig. 2). Although statistical relationships between soil properties and SAR backscatters changed with time, there was a significant correlation at the 0.05 level for all soil properties, except SOC in 60–100 cm. There were significant correlations

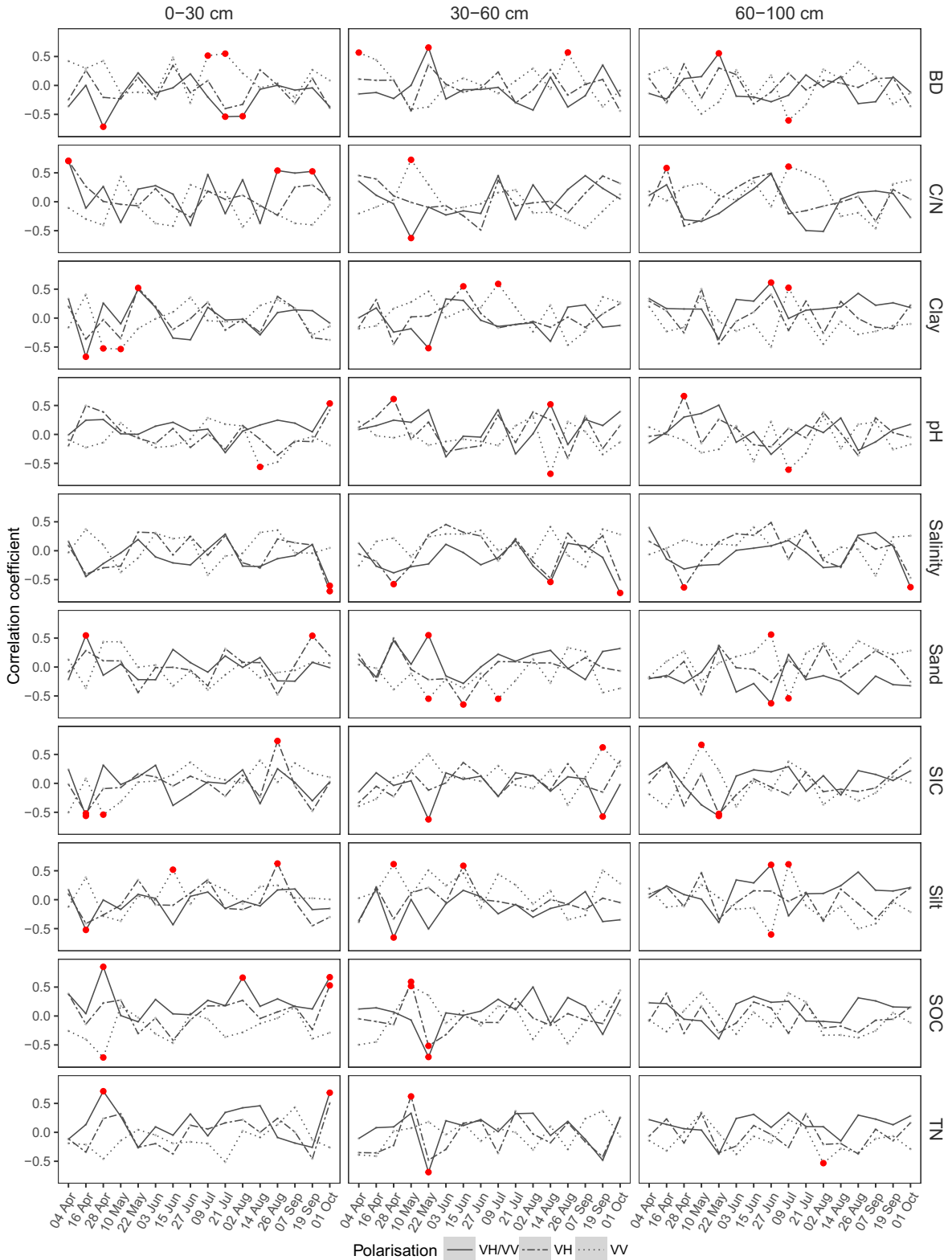

Fig. 3 Time-series plots of Pearson correlation coefficients between Sentinel-1 backscatters (VH, VV, and VH/VV) and soil properties. Red label indicates the significant correlation at the 0.05 level

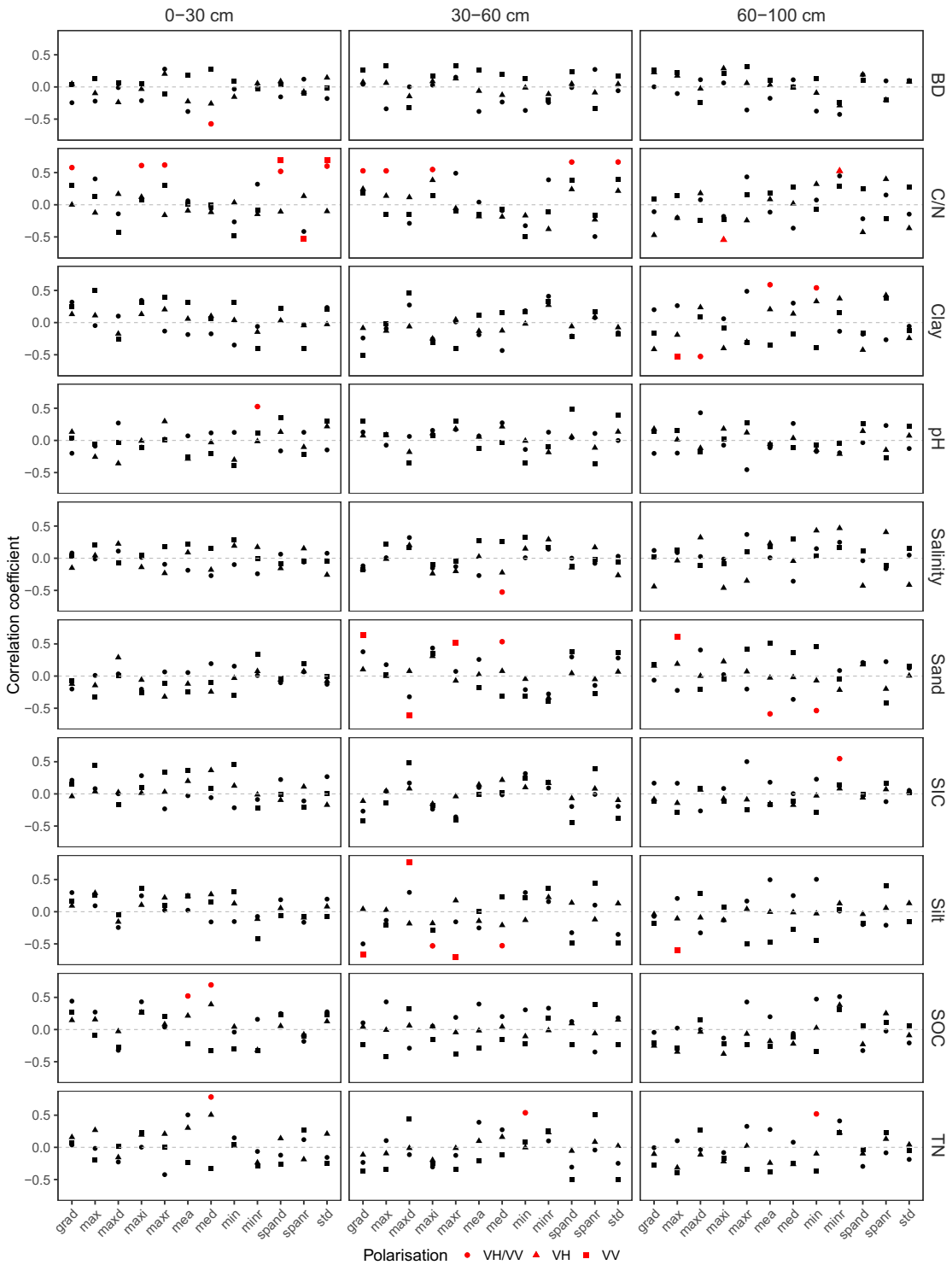

Fig. 4 Plots of Pearson correlation coefficients between multi-temporal features of Sentinel-1 data and soil properties. Red label indicates a significant correlation at the 0.05 level. Gradient (grad), maximum (max), maximum decrement (maxd), maximum increment (maxi), maximum ratio (maxr), mean (mea), median (med), minimum (min), minimum ratio (minr), span difference (spand), span ratio (spanr), and standard deviation (std)

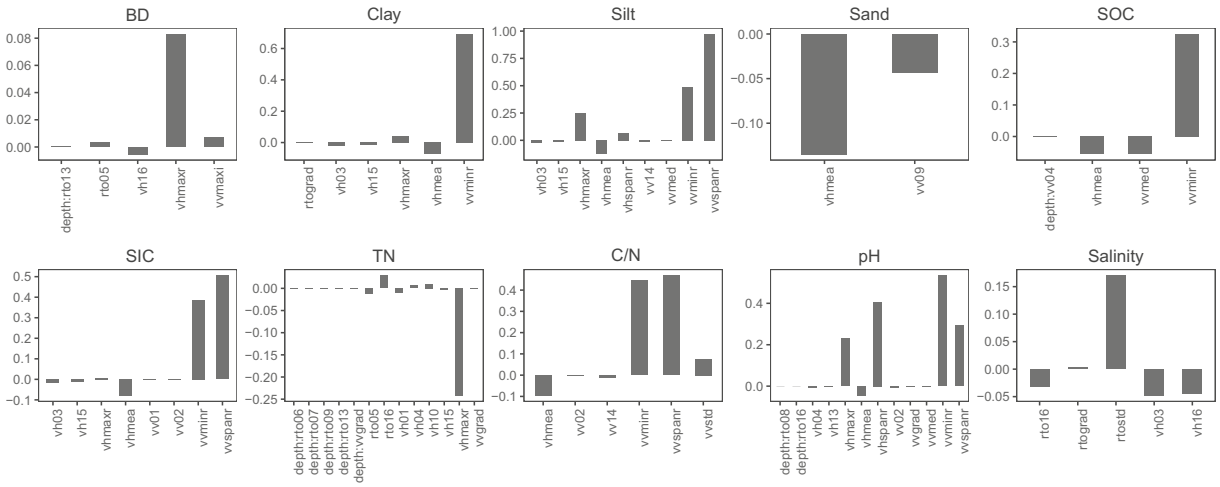

Fig. 5 Regression coefficients of 3D lasso models of soil properties. "rto" is "VH/VV"

between VH/VV backscatter and all soil properties in 0–30 and 30–60 cm, and BD, sand, silt, clay, SIC, and salinity in 60–100 cm, whereas there were fewer significant correlations relating VH and VV backscatters with soil properties. It indicates that VH/VV had a more powerful capability in indicating the spatial variation of soil than VH and VV, due to more sensitivity to vegetation. We observed that NDVI and VH/VV profiles in good agreement from 27 Jun to 28 Aug. This finding highlights the potential of VH/VV for plant

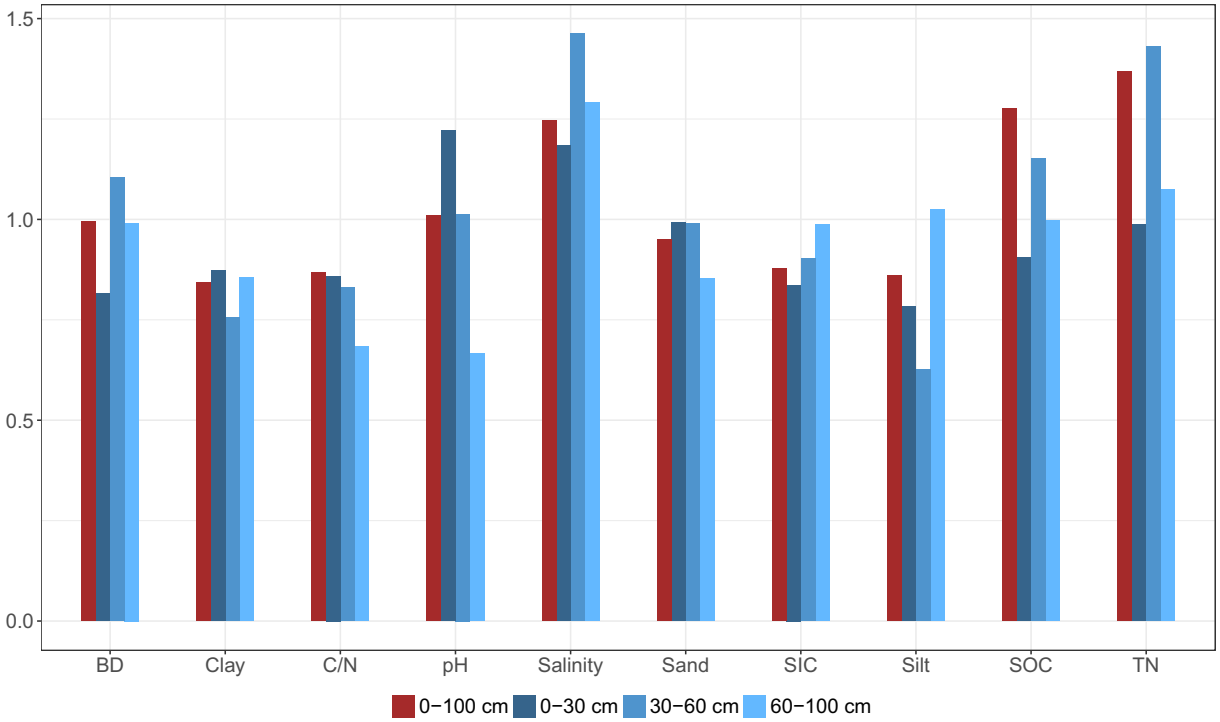

Fig. 6 Ratio of performance to deviation (RPD) values of 3D lasso models of soil properties based on leave-one-out cross-validation (LOOCV)

biomass detection. In general, VH/VV is likely to be linked to fresh biomass. Note that VH/VV could be used for estimating biophysical parameters and biomass assimilation due to the good agreement between NDVI and VH/VV, as found in Veloso et al. (2017).

During the growing season, characteristics of significant correlations between SAR backscatters and soil properties were observed, for similar soil properties: SOC and TN (VH/VV on 28 Apr and 01 Oct SOC for the top 30 cm, VH/VV and VH on 10 May and 22 May for 30–60 cm); also, pH and salinity (VH/VV on 01 Oct for 0–30 cm, VH on 28 Apr for 30–100 cm, and VH/VV on 14 Aug for 30–60 cm); lastly, soil texture (VH/VV on 16 Apr for the top 30 cm, VH on 15 Jun for 30–60 cm, and VH/VV on 27 Jun and VV on 09 Jul for 60–100 cm). These findings indicate that SAR backscatters can be associated with soil physicochemical properties related to soil depth. Because soil properties are indicators of soil functions and because a given soil function can be represented by different soil properties, some soil properties may share similar features captured by SAR data. For example, SOC and TN indicate functions of nutrient cycling and storage, and soil particles are the primary mineral forming blocks of soil. Soil pH and salinity are indicators representing functions of filtering and buffering. These results bring to light the valuable contribution of SAR indices for assessing soil functions.

Similar to the relationships between SAR backscatters and soil properties, variations of r values relating temporal features with soil properties were observed. However, there were less significant correlations between soil properties and temporal features than backscatters, indicating temporal features had a weaker capability in explaining spatial variations of soil than the backscatter measurements. For example, no significant correlations were observed for clay, sand, silt, salinity, and SIC in the top 30 cm. Temporal features, which were derived from VH/VV backscatters, were more sensitive to spatial variations of soil than that of VH and VV backscatters, confirming that VH/VV in this context was more useful comparing to VH and VV.

Modeling soil properties

Figure 5 presents the important predictors identified by 3D lasso models. A large number of variables were not used at all, indicating that the size of the predictors was efficiently reduced by lasso models. The regularization effect of lasso is able to not only improve prediction accuracy but also improve the model interpretability (Tibshirani et al. 2015). For this study, the important covariates applied in the models were different for predicting soil properties. For example, the most important associations with BD prediction were found with "VHmaxr," "VVmaxi," "VH16," "VH/VV05," and the interaction between "VH/VV13" and depth, while SOC was predicted from four predictors including "VVminr," "VVmed," "VHmea," and the interaction between "VV04" and depth. The diversity set of predictors can be attributed to the sensitivity of soil properties to SAR indices, which was indicated by the varying correlations between soil properties and SAR indices (as discussed above). Therefore, it is expected to examine temporal characteristics of SAR data, since more powerful indications of soil properties can be provided by time-series images other than a single phase.

Figure 6 presents RPD values of LOOCV results. The results showed that the overall prediction accuracy in the upper 1-m depth is permissible, with an average RPD value of 0.99. This finding demonstrated that in coastal wetlands, soil physicochemical properties can be successfully modeled using time-series SAR information, although there were temporal variations of the remote sensing signal. However, these models varied substantially in regarding RPD values, indicating the predictive capacity of SAR imagery differed among soil attributes. The observed indicative capacity of SAR data for soil physical properties had been found in previous studies (e.g., Ulaby et al. 1978; Santanello et al. 2007; Han et al. 2017). So far, few studies have been conducted for predicting soil chemical properties using SAR data, primarily using time-series characteristics of vegetation from SAR data. The successful applications of SAR data in relating soil chemical properties illustrate the potential of time-series SAR data for the retrieval of soil chemical properties.

Compared with SAR data, more effects have been made to predict soil properties using imaging spectroscopy data. In addition, previous studies mainly focused on a limited number of soil properties such as soil salinity, water content, and organic matter. For example, Zhang et al. (2011) found that soil salinity can be indirectly predicted using vegetation indices derived from hyperspectral data. Our study demonstrated that a variety set of soil properties can be indirectly predicted in a salt marsh environment using time-series Sentinel-1 imagery. Typically, soil properties could be associated with vegetation canopy detected from

satellite remote sensing data in coastal wetlands environments, because soils are strongly influenced by plant species that can be captured from remote sensing data (Anne et al. 2014). Zhang et al. (2019) indirectly quantified tidal marsh soil properties linked to plant patterns using imaging spectroscopy with acceptable prediction accuracy.

Our results also highlighted that models vary with the difference in predictive accuracy. As expected, higher accuracy can be achieved for soil properties related to nutrient and organic carbon storage. These soil properties were observed to be substantially influenced by *S. alterniflora* invasion. In other words, predictive accuracy may somewhat depend on the temporal variability of soil properties. Compared with soil chemical properties, physical properties may change slowly in response to *S. alterniflora* invasion (Yang and Guo 2018). In coastal wetlands of the East China Sea, *S. alterniflora* invasion substantially influenced vegetation characteristics such as the density, community, and structure (Li et al. 2009). In response, soil properties are thought to change due to the altered biogeochemical and physical processes induced by *S. alterniflora* invasion. For example, increasing above- and below-ground biomass affected the quantity and quality of C input in soils which is likely to have significant impacts on nutrient and carbon storage (Gao et al. 2016). Yang and Guo (2018) investigated the impacts of *S. alterniflora* on a set of soil physicochemical properties related to soil depth within 17-year invasion. They found that SOC storage, soil pH, and soil salinity were significantly correlated with the age of *S. alterniflora*, while soil physical properties were not significantly altered (i.e., soil texture, bulk density). Recent studies indicated that *S. alterniflora* invasion presents greater influence on soil biogeochemical services such as nutrient cycling and C sequestration (Wang et al. 2016a). As a result, soil changes in chemical properties are likely to be predicted with higher accuracy than soil physical properties.

Implications

In this study, we have focused on the question of "Does time-series Sentinel-1 data can indicate spatial variation of soil physicochemical properties in relation to depths through accounting variation of vegetation canopy?" Base on statistical analyses of relationships between Sentinel-1 data and soil properties, we can pose prospective attitudes toward soil prediction through SAR data in coastal wetlands with natural vegetation. Vegetation is an important factor that influences soil-forming processes, and thus it is theorized to regulate spatial variability of soil properties (Jenny 1941). Especially in invaded coastal ecosystems, invasion-related impacts to soil, for instance, carbon sequestration and salinization, are significant due to the critical influence nonnative species have on soil functions (Yang and Guo 2018). For a variety of reasons, including coastal sustainable management and soil protection, new strategies to investigate soil spatial variations are quite necessary. The findings of this study showed considerable correlations between SAR indices and a varied set of soil properties during a growing season, although there were weak and fluctuant correlations. Furthermore, the permissible prediction accuracy derived from 3D lasso models showed that time-series Sentinel-1 data has the capacity to indicate the variation of soil properties in lateral and vertical dimensions. The achievement of this study provided an important insight into the potential utility of SAR data for predicting a diverse set of soil properties from vegetation-covered soils. Due to the increasing availability of remote sensing data in high spatial-temporal resolution, soil prediction may become more readily accessible. Further studies are needed to focus on improving prediction accuracy using SAR data.

Conclusions

This study presents an assessment of temporal features of vegetation for estimating soil physicochemical properties using Sentinel-1 data in coastal wetlands. Our analysis showed that soil physicochemical properties can be modeled successfully with time-series SAR information. The analysis of time-series characteristics of three polarization channels presented that time-series Sentinel-1 data can capture temporal characteristics of vegetation, and VH/VV is more sensitivity to the vegetation growth than VH and VV. The understanding of temporal behaviors of SAR backscatters allows relating SAR information with soil properties. Significant correlations between SAR indices and soil properties related to soil depth can be observed during the growing season. The soil-vegetation relationship captured by time-series SAR data was beneficial to predict soil properties, especially

for soil chemical properties. Results also show that the application of the Sentinel-1 time-series data provides a practical solution for soil monitoring in coastal wetlands. We recommended using Sentinel-1-like data to predict soil physicochemical properties, regarding the advantage of the dense temporal information.

Funding information This research was supported by the National Natural Science Foundation of China (No. 41701236), the Natural Science Foundation of the Jiangsu Higher Education Institutions of China (No. 17KJB210004), and the Priority Academic Program Development of Jiangsu Higher Education Institutions.

References

Adhikari, K., Hartemink, A. E., Minasny, B., Kheir, R. B., Greve, M. B., & Greve, M. H. (2014). Digital mapping of soil organic carbon contents and stocks in Denmark. *PLoS One, 9*, e105519.

Anne, N. J., Abd-Elrahman, A. H., Lewis, D. B., & Hewitt, N. A. (2014). Modeling soil parameters using hyperspectral image reflectance in subtropical coastal wetlands. *International Journal of Applied Earth Observations, 33*, 47–56.

Araya, S., Lyle, G., Lewis, M., & Ostendorf, B. (2016). Phenologic metrics derived from MODIS NDVI as indicators for plant available water-holding capacity. *Ecological Indicators, 60*, 1263–1272.

Attema, E., Bargellini, P., Edwards, P., Levrini, G., Lokas, S., Moeller, L., et al. (2007). Sentinel-1-the radar mission for GMES operational land and sea services. *ESA Bulletin, 131*, 10–17.

Batjes, N. H. (1996). Total carbon and nitrogen in the soils of the world. *European Journal of Soil Science, 47*, 151–163.

Berkowitz, J. F., Van Zomeren, C. M., Piercy, C. D., & White, J. R. (2018). Evaluation of coastal wetland soil properties in a degradation marsh. *Estuarine, Coastal and Shelf Science, 212*, 311–317.

Brown, S. C., Quegan, S., Morrison, K., Bennett, J. C., & Cookmartin, G. (2003). High-resolution measurements of scattering in wheat canopies-implications for crop parameter retrieval. *IEEE Transactions on Geoscience and Remote Sensing, 41*, 1602–1610.

Demattê, J. A., Sayão, V. M., Rizzo, R., & Fongaro, C. T. (2017). Soil class and attribute dynamics and their relationship with natural vegetation based on satellite remote sensing. *Geoderma, 302*, 39–51.

Dubois, P. C., Van Zyl, J., & Engman, T. (1995). Measuring soil moisture with imaging radars. *IEEE Transactions on Geoscience and Remote Sensing, 33*, 915–926.

ESA. (2017). The sentinel application platform (SNAP), a common architecture for all sentinel toolboxes being jointly developed by Brockmann consult, array systems computing and C-S. http://step.esa.int/main/download/snap-download/. European Space Agency (ESA).

Feng, J., Zhou, J., Wang, L., Cui, X., Ning, C., Wu, H., Zhu, X., & Lin, G. (2017). Effects of short-term invasion of Spartina alterniflora and the subsequent restoration of native mangroves on the soil organic carbon, nitrogen and phosphorus stock. *Chemosphere, 184*, 774–783.

Freeman, A., & Durden, S. L. (1998). A three-component scattering model for polarimetric SAR data. *IEEE Transactions on Geoscience and Remote Sensing, 36*, 963–973.

Friedman, J., Hastie, T., & Tibshirani, R. (2010). Regularization paths for generalized linear models via coordinate descent. *Journal of Statistical Software, 33*, 1–22.

Gao, J. H., Feng, Z. X., Chen, L., Wang, Y. P., Bai, F., & Li, J. (2016). The effect of biomass variations of Spartina alterniflora on the organic carbon content and composition of a salt marsh in northern Jiangsu Province, China. *Ecological Engineering, 95*, 160–170.

Gedan, K. B., Silliman, B. R., & Bertness, M. D. (2009). Centuries of human-driven change in salt marsh ecosystems. *Annual Review of Marine Science, 1*, 117–141.

Han, D., Vahedifard, F., & Aanstoos, J. V. (2017). Investigating the correlation between radar backscatter and in situ soil property measurements. *International Journal of Applied Earth Observations, 57*, 136–144.

Hastie, T., Tibshirani, R., & Friedman, J. (2009). *The elements of statistical learning; data mining*. New York: Inference and Prediction, Springer.

IUSS Working Group WRB. (2015). World reference base for soil resources 2014: International soil classification system for naming soils and creating legends for SoilMaps: Update 2015. Rome.

Jenny, H. (1941). *Factors of soil formation: a system of quantitative pedology*. New York: McGraw-Hill.

Jia, M., Tong, L., Zhang, Y., & Chen, Y. (2013). Multitemporal radar backscattering measurement of wheat fields using multifrequency (L, S, C, and X) and full-polarization. *Radio Science, 48*, 471–481.

Jobbagy, E. G., & Jackson, R. B. (2000). The vertical distribution of soil organic carbon and its relation to climate and vegetation. *Ecological Applications, 10*, 423–436.

Kasischke, E. S., Melack, J. M., & Dobson, M. C. (1997). The use of imaging radars for ecological applications-a review. *Remote Sensing of Environment, 59*, 141–156.

Li, B., Liao, C. H., Zhang, X. D., Chen, H. L., Wang, Q., Chen, Z. Y., Gan, X. J., Wu, J. H., Zhao, B., Ma, Z. J., Cheng, X. L., Jiang, L. F., & Chen, J. K. (2009). Spartina alterniflora invasions in the Yangtze River estuary, China: an overview of current status and ecosystem effects. *Ecological Engineering, 35*, 511–520.

Liddicoat, C., Maschmedt, D., Clifford, D., Searle, R., Herrmann, T., Macdonald, L. M., & Baldock, J. (2015). Predictive mapping of soil organic carbon stocks in South Australia's agricultural zone. *Soil Research, 53*, 956–973.

Meersmans, J., van Wesemael, B., De Ridder, F., & van Molle, M. (2009). Modelling the three-dimensional spatial distribution of soil organic carbon (SOC) at the regional scale (Flanders, Belgium). *Geoderma, 152*, 43–52.

Metternicht, G. I., & Zinck, J. (2003). Remote sensing of soil salinity: potentials and constraints. *Remote Sensing of Environment, 85*, 1–20.

Minasny, B., McBratney, A., Malone, B., & Wheeler, I. (2013). Digital mapping of soil carbon. *Advances in Agronomy, 118*, 1–47.

Mishra, U., Lal, R., Slater, B., Calhoun, F., Liu, D. S., & van Meirvenne, M. (2009). Predicting soil organic carbon stock using profile depth distribution functions and ordinary kriging. *Soil Science Society of America Journal, 73*, 614–621.

Mulder, V., De Bruin, S., Schaepman, M., & Mayr, T. (2011). The use of remote sensing in soil and terrain mapping-a review. *Geoderma, 162*, 1–19.

Nelson, D., & Sommers, L. E. (1982). Total carbon, organic carbon, and organic matter. In R. W. Weaver (Ed.), *Methods of soil analysis part 2: chemical and microbiological properties* (pp. 539–579). Madison: American Society of Agronomy.

Nussbaum, M., Spiess, K., Baltensweiler, A., Grob, U., Keller, A., Greiner, L., Schaepman, M. E., & Papritz, A. (2018). Evaluation of digital soil mapping approaches with large sets of environmental covariates. *Soil, 4*, 1–22.

Pejović, M., Nikolić, M., Heuvelink, G. B., Hengl, T., Kilibarda, M., & Bajat, B. (2018). Sparse regression interaction models for spatial prediction of soil properties in 3D. *Computers & Geosciences, 118*, 1–13.

Poggio, L., & Gimona, A. (2014). National scale 3D modelling of soil organic carbon stocks with uncertainty propagation - an example from Scotland. *Geoderma, 232-234*, 284–299.

R Core Team. (2017). *R: a language and environment for statistical computing*. Vienna.

Rhoades, J., & Ingvalson, R. (1971). Determining salinity in field soils with soil resistance measurements 1. *Soil Science Society of America Journal, 35*, 54–60.

Santanello, J. A., Peters-Lidard, C. D., Garcia, M. E., Mocko, D. M., Tischler, M. A., Moran, M. S., et al. (2007). Using remotely-sensed estimates of soil moisture to infer soil texture and hydraulic properties across a semi-arid watershed. *Remote Sensing of Environment, 110*, 79–97.

Sarti, M., Migliaccio, M., Nunziata, F., Mascolo, L., & Brugnoli, E. (2017). On the sensitivity of polarimetric SAR measurements to vegetation cover: the Coiba National Park, Panama. *International Journal of Remote Sensing, 38*, 6755–6768.

Schuler, D. L., Lee, J. S., Kasilingam, D., & Nesti, G. (2002). Surface roughness and slope measurements using polarimetric SAR data. *IEEE Transactions on Geoscience and Remote Sensing, 40*, 687–698.

Sherrod, L., Dunn, G., Peterson, G., & Kolberg, R. (2002). Inorganic carbon analysis by modified pressure-calcimeter method. *Soil Science Society of America Journal, 66*, 299–305.

Solon, J., Roo-Zielińska, E., & Degorski, M. (2012). Landscape scale of topography-soil-vegetation relationship: influence of land use and land form. *Polish Journal of Ecology, 60*, 3–17.

Srivastava, H. S., Parul, P., & Ranganath, R. N. (2006). How far SAR has fulfilled its expectation for soil moisture retrieval. In *Microwave remote sensing of the atmosphere and environment* (Vol. 6410). Bellingham: International Society for Optics and Photonics.

Tibshirani, R. (1996). Regression shrinkage and selection via the lasso. *Journal of the Royal Statistical Society Series B, 58*, 267–288.

Tibshirani, R., Wainwright, M., & Hastie, T. (2015). *Statistical learning with sparsity: the lasso and generalizations*. Boca Raton: Chapman and Hall/CRC.

Ulaby, F. T., Batlivala, P. P., & Dobson, M. C. (1978). Microwave backscatter dependence on surface roughness, soil moisture, and soil texture: part I-bare soil. *IEEE Transactions on Geoscience Electronics, 16*, 286–295.

Vaudour, E., Bel, L., Gilliot, J. M., Coquet, Y., Hadjar, D., Cambier, P., Michelin, J., & Houot, S. (2013). Potential of SPOT multispectral satellite images for mapping topsoil organic carbon content over peri-urban croplands. *Soil Science Society of America Journal, 77*, 2122–2139.

Veloso, A., Mermoz, S., Bouvet, A., Le Toan, T., Planells, M., Dejoux, J. F., et al. (2017). Understanding the temporal behavior of crops using Sentinel-1 and Sentinel-2-like data for agricultural applications. *Remote Sensing of Environment, 199*, 415–426.

Veronesi, F., Corstanje, R., & Mayr, T. (2014). Landscape scale estimation of soil carbon stock using 3D modelling. *Science of the Total Environment, 487*, 578–586.

Wang, C., Pei, X., Yue, S., & Wen, Y. (2016a). The response of Spartina alterniflora biomass to soil factors in Yancheng, Jiangsu Province, PR China. *Wetlands, 36*, 229–235.

Wang, H. Q., Piazza, S. C., Sharp, L. A., Stagg, C. L., Couvillion, B. R., Steyer, G. D., et al. (2016b). Determining the spatial variability of wetland soil bulk density, organic matter, and the conversion factor between organic matter and organic carbon across Coastal Louisiana, U.S.A. *Journal of Coastal Research, 33*, 507–517.

Yang, R. M., & Guo, W. W. (2018). Exotic *Spartina alterniflora* enhances the soil functions of a coastal ecosystem. *Soil Science Society of America Journal, 92*, 901–909.

Yang, R. M., Rossiter, D. G., Liu, F., Lu, Y., Yang, F., Yang, F., et al. (2015). Predictive mapping of topsoil organic carbon in an alpine environment aided by Landsat TM. *PLoS One, 10*, e0139042.

Yang, W., Zhao, H., Leng, X., Cheng, X., & An, S. (2017). Soil organic carbon and nitrogen dynamics following *Spartina alterniflora* invasion in a coastal wetland of eastern China. *Catena, 156*, 281–289.

Yuan, J. J., Ding, W. X., Liu, D. Y., Kang, H., Freeman, C., Xiang, J., et al. (2015). Exotic *Spartina alterniflora* invasion alters ecosystem-atmosphere exchange of CH4 and N2O and carbon sequestration in a coastal salt marsh in China. *Global Change Biology, 21*, 1567–1580.

Zhang, T. T., Zeng, S., Gao, Y., Ouyang, Z., Li, B., Fang, C., & Zhao, B. (2011). Using hyperspectral vegetation indices as a proxy to monitor soil salinity. *Ecological Indicators, 11*, 1552–1562.

Zhang, C., Mishra, D. K., & Pennings, S. C. (2019). Mapping salt marsh soil properties using imaging spectroscopy. *ISPRS Journal of Photogrammetry and Remote Sensing, 148*, 221–234.

Publisher's note Springer Nature remains neutral with regard to jurisdictional claims in published maps and institutional affiliations.